ChemComm

An Optimal Trapdoor Zeolite for Exclusive Admission of CO2 at Industrial Carbon Capture Operating Temperatures

Journal:	*ChemComm*
Manuscript ID	CC-COM-01-2018-000634.R1
Article Type:	Communication

ChemComm

COMMUNICATION

An Optimal Trapdoor Zeolite for Exclusive Admission of CO_2 at Industrial Carbon Capture Operating Temperatures†

Received 00th January 20xx,
Accepted 00th January 20xx

DOI: 10.1039/x0xx00000x

www.rsc.org/

Tao Du,[a] Xin Fang,[ab] Liying Liu,*[ac] Jin Shang,[d] Bin Zhang,[a] Yichao Wei,[a] He Gong,[a] Shamsur Rahman,[c] Eric F. May,[c] Paul A. Webley[b] and Gang (Kevin) Li*[bc]

High purity molecular trapdoor chabazite with an optimal Si/Al ratio (1.9) was prepared from fly ash. Gas adsorption isotherms and binary breakthrough experiments show dramatically large selectivities for CO_2 over N_2 and CH_4, among the highest for physisorbents at operating temperatures suitable for postcombution carbon capture and natural gas separations.

Adsorption based separation of carbon dioxide from important industrial gas mixtures such as flue gas and natural gas has gained worldwide research interest owing to increased environmental and economic incentives.[1-3] High CO_2 selectivity and low manufacture cost are key attributes of any new carbon capture adsorbents that receive consideration by industry. Conventionally, selectivity in physisorption (the preferred regime due to low energy consumption for regeneration) depends on three separation mechanisms, namely equilibrium,[4] kinetic,[5] and steric.[6] Carbon dioxide has large multi-poles and appreciable polarizability and is therefore able to bind preferentially to adsorbents, resulting in a higher equilibrium capacity than that can be achieved by other light components such as N_2 and CH_4.[7] However, equilibrium selectivity is often limited and rapidly reduces with increasing pressure because of the linear uptake of the light components compared with the early saturation of the heavy one.[1] Likewise, kinetic separations frequently suffer from reduced mass transfer rates and compromised bed capacity due to short cycle times. Steric, i.e., size and/or shape sieving may in principle achieve perfect separations but are often simply not available when the size difference between the two molecules is negligible.[8]

In contrast, a new “molecular trapdoor” physisorption mechanism,[2] which was recently discovered in small pore zeolites, provides an alternative pathway for developing ultra-high selective adsorbents. The molecular trapdoor mechanism in small pore zeolites, such as K-CHA, Cs-CHA, and RHO, refers to the ability of certain gas molecules to reversibly and temporarily open 8MRs (eight-membered oxygen rings), which are otherwise blocked by a cation, thereby permitting the entrance of the guest molecule into the zeolite supercage though a ~0.38×0.38 nm aperture.[2,8] In particular, guest molecules (such as CO_2) which have a relatively strong interaction with the door-keeping cations are able to enter the zeolite supercage as shown in Figure 1a, whereas molecules with weak interactions (such as N_2 or CH_4) are excluded because they do not perturb the cation sufficiently. As a consequence, record high selectivities of 93 for CO_2/CH_4 separation and 80 for CO_2/N_2 separation were achieved at 273 K and 100 kPa with a pseudo-**r1**KCHA trapdoor zeolite (i.e. potassium chabazite with a nominal Si/Al ratio of 1, see Figure S1 in ESI) in 2012.[2] However, the effective selectivity achievable in a swing-adsorption process can be limited at higher temperatures because, above a certain threshold admission temperature T_0, the cation’s increased thermal energy means it can also be displaced temporarily by guest molecules with weaker interaction energies. Recent process demonstrations using pressure swing adsorption (PSA) technology for carbon capture with kilogram-scale trapdoor chabazites indicated that CO_2 recovery and purity dropped dramatically above 291 K column temperature using an **r2.2**KCHA.[9] Given the adsorption step of a PSA cycle is strongly exothermic due to its adiabatic operation[10,11] and real postcombustion carbon capture processes must deal with hot flue gases (up to 363 K even after equipping the waste heat recovery unit), there is a strong need to develop a trapdoor zeolite that can exclusively adsorb CO_2 at industrial carbon capture operating temperatures.

The main objective of this work is to find such a trapdoor zeolite: one that rejects N_2 and CH_4 but adsorbs CO_2 with a working temperature suitable for postcombustion carbon

---

[a] State Environmental Protection Key Laboratory of Eco-Industry, School of Metallurgy, Northeastern University, Shenyang, 110819, China. E-mail: liuly@smm.neu.edu.au

[b] Department of Chemical Engineering, The University of Melbourne, Melbourne, Victoria 3010, Australia. E-mail: li.g@unimelb.edu.au

[c] ARC Centre for LNG Futures, The University of Western Australia, 35 Stirling Highway, Crawley, Western Australia 6009, Australia.

[d] Joint Laboratory for Energy and Environmental Catalysis, School of Energy and Environment, City University of Hong Kong, Hong Kong SAR, China.

†Electronic Supplementary Information (ESI) available: For DFT calculations, experiments and other supporting information see DOI: 10.1039/x0xx00000x.

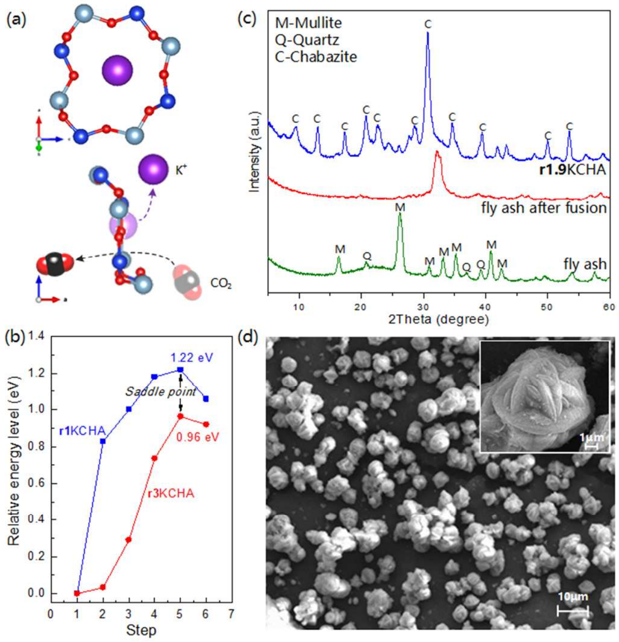

Figure 1 (a) The front view of the 8MR (top) and the movement of door-keeping potassium cation during CO_2 adsorption (side view, bottom). (b) Energy profiles for the potassium cation of **r1**KCHA and **r3**KCHA. (c) XRD patterns of the raw fly ash, intermediate, and resultant **r1.9**CHA. (d) SEM images for **r1.9**KCHA.

capture and natural gas separations, e.g. from sub-ambient up to the temperature of flue gases.

Our strategy for developing such a trapdoor zeolite is to elevate the threshold admission temperatures of CH_4 and N_2 by increasing the energy barriers ΔE required for the passage of guest molecule through the cation blocked 8MR doorway. Here we use density functional theory (DFT) calculations to demonstrate that the ΔE for a given gas-zeolite system has a strong dependence on the density of cations in the trapdoor zeolite (see DFT calculations section in ESI for detailed procedure). In a typical potassium chabazite system (see Figure S2 for the 3D structure),[12] we studied the admission process of CO_2 gas in two scenarios with different Si/Al ratios, namely 3 and 1; the corresponding chabazites are denoted as **r3**KCHA and **r1**KCHA, respectively (Figure S3). Lower Si/Al ratios have higher cation densities to ensure charge balance. As shown in Figure 1b, the admission energy barrier of ΔE(CO_2-**r3**KCHA) is 22% lower than that of ΔE(CO_2-**r1**KCHA). This is because the higher density of cations in the chabazite supercage substantially increases the space hindrance and repulsion for the movement of the door-keeping cation and the guest molecule. Furthermore, the high negative charge density on the aluminosilicate framework makes the cations less mobile. It could thus be expected that reducing the Si/Al ratio in KCHA would increase the threshold admission temperature T_0. In a typical **r2.2**KCHA, T_0 for CH_4 and N_2 is 266 K and 254 K, respectively.[3] However, attempts to produce functional trapdoor chabazites with Si/Al ratios below 2 were not successful due to inherent drawbacks of the prior synthesis method[13] in which alumina hydroxide slurry was used to enrich the Al content of the chabazite and, consequently, the occurrence of inhomogeneous Si → Al exchange and the presence of amorphous alumina in the product are unavoidable.

Herein, we report an ultra-low Si trapdoor chabazite (Si/Al = 1.9) with unparalleled CO_2/CH_4 and CO_2/N_2 adsorption selectivity at temperatures measured up to 348 K relevant to industrial practice. Importantly, this **r1.9**KCHA was synthesized from coal fly ash through a template-free hydrothermal method which is very different from conventional procedures reported by others using either organic structure-directing agents or inter-zeolite conversion from Y precursers.[14,15] Briefly, selected fly ash with Si and Al content close to low-silica chabazite was reacted with excessive KOH powder through a high temperature fusion process at 923 K for 1 h to break up mullite and quartz phases (Figure 1c). The resultant mixture was treated under hydrothermal conditions for 4 days to produce the target **r1.9**KCHA (see Experiments section in ESI for complete procedure).

The morphology and structure of the starting material and the end product were examined by scanning electron microscope (SEM) and X-ray diffraction (XRD), respectively. As shown in Figure S4, the fly ash is comprised of particles with a wide size distribution from sub-micron to 30 micron, with shapes varying from spherical beads, to irregular lumps and short needles, which is attributable to mullite and quartz, according to the literature[16] and their characteristic XRD patterns (Figure 1c). In contrast, the as-synthesized chabazite (Figure 1d) derived from fly ash presents a walnut-like shape with a uniform diameter of approximately 2-5 micron[14]. High resolution SEM (Figure 1d) reveals the "walnuts" are intergrown multi-crystals of chabazite. It is worth mentioning that the morphology of our chabazite is quite different from those produced previously through intercrystal conversion processes[17] which exhibited a similar morphology to the precursor zeolite Y. Very little amorphous material was observed in the SEM images of the fly ash-derived chabazite. A high purity, highly crystalline

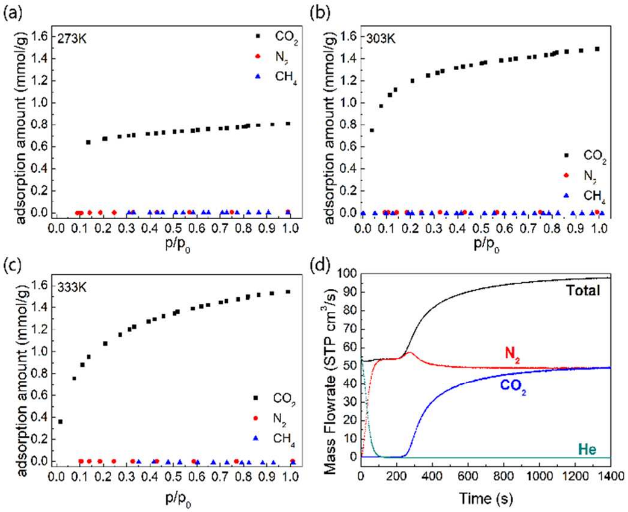

Figure 2 CO_2, N_2 and CH_4 adsorption isotherms on **r1.9**KCHA at (a) 273, (b) 303 and (c) 333 K, and (d) breakthrough curve for equimolar binary CO_2/N_2 on **r1.9**KCHA at 348 K and total pressure of 1 bar.

chabazite phase was clearly evidenced by the characteristic XRD patterns (Figure 1c).

The Si/Al ratio of the as-synthesized chabazite was verified to be 1.9 by XRF analysis. Apart from the dominant potassium, other metallic minor components from the fly ash were also partially retained in the chabazite giving a product composition of $K_{9.79}Fe_{0.44}Ca_{0.57}Al_{12.25}Si_{23.75}O_{72}$, suggesting the product chabazite has very minor mixed cations. Note that potassium is an effective door-keeping cation in chabazite, and the minimum number of potassium cations required for a chabazite to exhibit the trapdoor effect is 9 per unit cell corresponding to Si/Al = 3,[2] which is below the number in the chabazite synthesized from this work.

The adsorption properties of our **r1.9**KCHA were analysed with single component measurements of N_2, CH_4 and CO_2 and summarized in Figure 2a-c. The N_2 adsorption on this chabazite at 77 K was found to be close to that of nonporous powdered materials, giving rise to a negligible BET surface area, which is typical to trapdoor zeolites. At temperatures of 273, 303 and 333 K, the adsorption of both N_2 and CH_4 still remained negligible, with uptake signals falling into the noise level of the measurement instrument (ASAP 2010, Micromeritics). Even at 333 K and 100 kPa, the adsorption capacities of N_2 and CH_4 on **r1.9**KCHA are still below 0.02 mmol/g, which is about 25-30 times smaller than those for **r2.2**KCHA reported in our earlier work,[2] indicating the threshold admission temperature T_0 for N_2 and CH_4 have been substantially elevated to above 343 K.

On the contrary, a considerable amount of CO_2 was adsorbed onto **r1.9**KCHA. At 100 kPa, the adsorption capacity at 273, 303 and 333 K was 0.81 mmol/g, 1.49 mmol/g, and 1.54 mmol/g, respectively. This trend of greater equilibrium capacities at higher temperatures is opposite to that of the normal Arrhenius type physisorption. However, the equilibrium adsorption of CO_2 does not increase indefinitely with temperature, peaking at around 333 K and then declining at higher temperatures. A "bell shaped" CO_2 adsorption isobar is observed as shown in Figure S5, which is a signature of the trapdoor effect previously reported for weakly-interacting molecules like CH_4 and N_2 in **r2.2**KCHA.[2,3] However, it is rare to see temperature-regulated admission of CO_2 molecules, because CO_2 is able to interact strongly with door-keeping cations due to its large quadrupole moment (13.4×10^{-40} cm^2) and polarizability (29.1×10^{-25} cm^{-3}). This observation implies that at sufficiently low temperatures it is possible to restrict the pore access of trapdoor zeolites even for strong molecules like CO_2. This effect could enable sieving-based processes for separating polar molecules.

Based on the single component adsorption isotherms, one might anticipate that the **r1.9**KCHA will exclusively adsorb all of the CO_2 but reject CH_4 and N_2 in a gas mixture in the corresponding temperature range. However, such extrapolations can be risky as multicomponent selectivity is not always guaranteed from equilibrium information of single components, regardless the model of prediction (e.g. IAST[18] or extended Langmuir).

To evaluate the real separation selectivity of CO_2 against CH_4 and N_2 on **r1.9**KCHA, multicomponent column breakthrough experiments were conducted using equimolar gas mixtures of CO_2/N_2 (or CH_4) with a feed flowrate of 100 sccm, at temperatures ranging from 303 up to 348 K, and at 1 and 3 bar. In a typical run, a stainless-steel column containing 25.8 g of tightly packed **r1.9**KCHA pellets (~1 mm in diameter) was initially flushed by He and, then switched to the flow of target gas mixtures at the same pressure. The gas composition and the mass flowrate at the outlet of the column were recorded as a function of elution time to give the so-called breakthrough curve (refer to Multicomponent breakthrough experiments section in ESI for details).[19,20] As shown by Figure 2d, instantaneous elution of N_2 occurred right after the gas switch along with the flush of the prefilled He, while CO_2 was detected at the outlet only after a substantially longer time (200 seconds), indicative of negligible loading of N_2 but a substantial uptake of CO_2. Remarkably, the measured CO_2/N_2 and CO_2/CH_4 selectivities for mixtures under these conditions are enormously large (summarized in Table S1), e.g. 688 for the case in Figure 2d, as determined from mass balance calculations, which are also consistent with predictions from single component isotherms.

In CO_2 capture applications, a high selectivity for CO_2 over the other components of the gas mixture is essential.[4] The performance of our chabazite derived from fly ash is compared

Table 1 Comparison of the performance of adsorbing materials with the highest reported CO_2 selectivities.

Compounds	Selectivity at 1 bar		CO_2 uptake @ P_{CO2} (mmol/g)	Temperature (K)	Ref.
	CO_2/CH_4	CO_2/N_2			
r1.9KCHA	**50/50, 583**[a]	**50/50,90 (303 K)**[a] **50/50,688 (348 K)**[a]	**1.01 (51 kPa, 303 K)** **0.83 (51 kPa, 348 K)**	**303~348**	**this work**
pseudo-**r1**KCHA[b]	15/85, 79[a]		1.59 (17.4 kPa)	293	2
r2CsCHA	15/85, 109[a]		1.63 (17.4 kPa)	293	2
MIL-53(Cr)	50/50, 3.2[a]		2.25 (500 kPa)	303	21
porph(Cl^-)@MOM-11(Mn^{2+})	50/50, 11.9[b]		2.86 (101 kPa)	298	22
CBZ	50/50, 13.2[b]	50/50, 100[c]	1.56 (51 kPa)	273	23
Mg-DOBDC		10/90, 235[c]	3.84 (10 kPa)	298	24
UTSA-16		10/90, 58[c]	1.86 (10 kPa)	298	24
HKUST-1		15/85, 101[c]	2.64 (15 kPa)	298	25
ZIF-78		15/85, 30[c]	0.75 (15 kPa)	298	26,27
mmen-Cu-BTTri		15/85, 165[c]	2.16 (15 kPa)	298	28

[a] selectivity obtained from breakthrough experiment, [b] impure CHA containing amorphous alumina, [c] selectivity calculated from single-component isotherms.

with other well-known CO_2 adsorbing materials in Table 1. However, many of the selectivities reported in literature are simply calculated from pure component adsorption isotherms. Data measured by multicomponent equilibrium adsorption experiments are little. Furthermore, CO_2/N_2 selectivities are frequently determined at or below 298 K. It would be more useful when assessing prospective adsorbents for postcombustion carbon capture processes, if their CO_2 over N_2 selectivity were assessed in the range of flue gas temperature (313-363 K). As shown in Table 1, the selectivities of CO_2 over N_2 and CH_4 on our **r1.9**KCHA are to the best of our knowledge the highest for CO_2 over N_2 and CH_4 among all physisorbents; moreover, the maximum selectivities were achieved at 348 K, within the temperature range of flue gas applications. With these uniquely high CO_2 selectivities, such fly ash derived chabazite would appear to be a supreme adsorbent for industrial CO_2/N_2 and CO_2/CH_4 separations.

In summary, we have successfully produced low silica trapdoor chabazites from fly ash. The resulting chabazite had a high crystallinity and a typical walnut-like shape morphology with a uniform size distribution. Multicomponent adsorption measurements showed dramatically large selectivities of CO_2 over N_2 and CH_4 on our chabazite, demonstrating ultra-high performance for the separation of CO_2 from flue gas and natural gas at industrial operating temperatures. Additionally, this work opens a new pathway of recycling fly ash for the manufacture of high value-added products.

The authors gratefully acknowledge the financial support of Natural Science Foundation of China (Grant Nos. 51474067 and 51406029) and the Education Department of Liaoning Province (Funding No. LZ2015032) and National Department of Education (Funding No. N150204015). G. Li is the recipient of an Australian Research Council Discovery Early Career Research Award (DE140101824). E. May, G. Li, P. Webley and L. Liu acknowledge the funding support of Australian Research Council through the Industrial Transformation Training Centre for Liquefied Natural Gas Futures (IC150100019).

Conflicts of interest

The authors declare no conflict of interest.

Notes and references

1 D. Saha and Z. Bao, *Environ. Sci. Technol.*, 2010, **44**, 1820–1826.
2 J. Shang, G. Li, R. Singh, Q. Gu, K. M. Nairn, T. J. Bastow, N. Medhekar, C. M. Doherty, A. J. Hill, J. Z. Liu and P. A. Webley, *J. Am. Chem. Soc.*, 2012, **134**, 19246–19253.
3 G. K. Li, J. Shang, Q. Gu, R. V Awati, N. Jensen, A. Grant, X. Zhang, D. S. Sholl, J. Z. Liu, P. A. Webley and E. F. May, *Nat. Commun.*, 2017, **8**, 15777.
4 K. Sumida, D. L. Rogow, J. A. Mason, T. M. McDonald, E. D. Bloch, Z. R. Herm, T. H. Bae and J. R. Long, Chem. Rev., 2012, **112**, 724–781.
5 M. Dinca and J. R. Long, *J. Am. Chem. Soc.*, 2005, **127**, 9376-9377.
6 W. Yuan, Y. S. Lin and W. Yang, *J. Am. Chem. Soc.*, 2004, **126**, 4776–4777.
7 J. Shang, G. Li, R. Singh, P. Xiao, D. Danaci, J. Z. Liu and P. A. Webley, *J. Chem. Phys.*, 2014, **140**, 084705.
8 M. T. S. M. Kuznicki, V.A. Bell, S. Nair, H.W. Hillhouse, R. M. Jacubinas, C.M. Braunbarth, B.H. Toby, *Nature*, 2001, **412**, 720–724.
9 P. A. Webley, in Seventh Pacific Basin Conference on Adsorption Science and Technology, Xiamen, 2015.
10 G. Li, P. Xiao, J. Zhang, P. A. Webley and D. Xu, *AIChE J.*, 2014, **60**, 673–689.
11 G. Li, P. Xiao, P. Webley, J. Zhang, R. Singh and M. Marshall, *Adsorption*, 2008, **14**, 415–422.
12 F. Göltl and J. Hafner, *J. Chem. Phys.*, 2011, **134**, 064102.
13 K. a. Thrush and S. M. Kuznicki, *J. Chem. Soc. Faraday Trans.*, 1991, **87**, 1031.
14 B. Liu, Y. Zheng, N. Hu, T. Gui, Y. Li, F. Zhang, R. Zhou, X. Chen and H. Kita, *Microporous Mesoporous Mater.*, 2014, **196**, 270–276.
15 US Pat. 4,503,024, 1985, US, 1–6.
16 L. Liu, R. Singh, G. Li, P. Xiao, P. Webley and Y. Zhai, *J. Hazard. Mater.*, 2011, **195**, 340–345.
17 J. Shang, G. Li, R. Singh, P. Xiao, J. Z. Liu and P. A. Webley, *J. Phys. Chem. C*, 2010, **114**, 22025–22031.
18 T. Van Heest, S. L. Teich-McGoldrick, J. A. Greathouse, M. D. Allendorf and D. S. Sholl, *J. Phys. Chem. C*, 2012, **116**, 13183–13195.
19 T. L. H. Saleman, G. C. Y. Watson, T. E. Rufford, P. S. Hofman, K. I. Chan and E. F. May, *Adsorption*, 2013, **19**, 1165–1180.
20 T. Saleman, G. Xiao, G. Li and E. F. May, *Adsorption*, 2017, **23**, 1-14.
21 L. Hamon, P. L. Llewellyn, T. Devic, A. Ghoufi, G. Clet, V. Guillerm, G. D. Pirngruber, G. Maurin, C. Serre, G. Driver, W. Van Beek, E. Jolimaître, A. Vimont, M. Daturi and G. Férey, *J. Am. Chem. Soc.*, 2009, **131**, 17490–17499.
22 Z. Zhang, W. Y. Gao, L. Wojtas, S. Ma, M. Eddaoudi and M. J. Zaworotko, *Angew. Chemie - Int. Ed.*, 2012, **51**, 9330–9334.
23 M. Saleh, H. M. Lee, K. C. Kemp and K. S. Kim, *ACS Appl. Mater. Interfaces*, 2014, **6**, 7325–7333.
24 S. J. Datta, C. Khumnoon, Z. H. Lee, W. K. Moon, S. Docao, T. H. Nguyen, I. C. Hwang, D. Moon, P. Oleynikov, O. Terasaki and K. B. Yoon, *Science*, 2015, **350**, 302–306.
25 P. Aprea, D. Caputo, N. Gargiulo, F. Iucolano and F. Pepe, *J. Chem. Eng. Data*, 2010, **55**, 3655–3661.
26 R. Banerjee, H. Furukawa, D. Britt, C. Knobler, M. O. Keeffe and O. M. Yaghi, *J. Am. Chem. Soc.*, 2009, **131**, 3875–3877.
27 A. Phan, C. J. Doonan, F. J. Uribe-Romo, C. B. Knobler, M. O'Keeffe and O. M. Yaghi, *Acc Chem Res*, 2010, **43**, 58–67.
28 T. M. McDonald, D. M. D'Alessandro, R. Krishna and J. R. Long, *Chem. Sci.*, 2011, **2**, 2022.